STATE RESEARCH CENTER OF RUSSIA

INSTITUTE FOR HIGH ENERGY PHYSICS

IHEP 97-56

FNAL E704 Collaboration

MEASUREMENT OF SINGLE SPIN ASYMMETRY IN η-MESON PRODUCTION IN $p_\uparrow p$- AND $\bar{p}_\uparrow p$-INTERACTIONS IN THE BEAM FRAGMENTATION REGION AT 200 GEV/C

Submitted to *Nuclear Physics B*

Protvino 1997

UDK 539.12.142 M–24

Abstract

FNAL E704 Collaboration. Measurement of single spin asymmetry in η-meson production in $p_\uparrow p$- and $\bar{p}_\uparrow p$-interactions in the beam fragmentation region at 200 GeV/c: IHEP Preprint 97-56. – Protvino, 1997. – p. 10, figs. 7, tables 4, refs.: 6.

We present experimental results on measuring a single spin asymmetry in η-meson production in the interaction of transversely polarized protons and antiprotons at $p_{\rm lab} = 200$ GeV/c with a proton target in the region $0.2 < x_F < 0.7$ for $p_\uparrow p$, $0.3 < x_F < 0.7$ for $\bar{p}_\uparrow p$ and $0.7 < p_T < 2.0$ GeV/c. Comparison of single spin asymmetries in π- and η-meson production is done.

Аннотация

Коллаборация E704, ФНАЛ. Измерение односпиновой асимметрии в образовании η-мезона в $p_\uparrow p$- и $\bar{p}_\uparrow p$-взаимодействиях в области фрагментации пучка при 200 ГэВ/с: Препринт ИФВЭ 97-56. – Протвино, 1997. – 10 с., 7 рис., 4 табл., библиогр.: 6.

Представлены экспериментальные результаты по измерению односпиновой асимметрии в образовании η-мезона во взаимодействиях поперечно поляризованных протонов и антипротонов при $p_{\rm lab} = 200$ ГэВ/с с протонной мишенью в области $0.2 < x_F < 0.7$ для $p_\uparrow p$, $0.3 < x_F < 0.7$ для $\bar{p}_\uparrow p$ и $0.7 < p_T < 2.0$ ГэВ/с. Дается сравнение односпиновых асимметрий в образовании π- и η-мезонов.

Introduction

The experiment E704 was carried out at FNAL and was devoted to the study of polarization effects in $p_\uparrow p$ and $\bar{p}_\uparrow p$ collisions with transversely and longitudinally polarized proton and antiproton beams at $p_{\rm lab} = 200$ GeV/c. Significant single spin asymmetries were observed by this experiment in π^0 [1], $\pi^\pm$ [2] and Λ [3] production in the fragmentation region of the polarized beams. Now we present the measurements of the x_F-dependence of the single spin asymmetries A_N for the reactions

$$p_\uparrow p \;\rightarrow\; \eta X \tag{1}$$

$$\bar{p}_\uparrow p \;\rightarrow\; \eta X, \tag{2}$$

performed in the region $0.2 < x_F < 0.7$ for reaction (1), $0.3 < x_F < 0.7$ for reaction (2) and $0.7 < p_T < 2.0$ GeV/c for both reactions. The transverse single spin asymmetry is determined [4] as a relative difference of cross sections of particle production to the left with up and down alignment of the beam polarization:

$$A_N = \frac{1}{P_{\rm b}} \frac{d\sigma_\uparrow - d\sigma_\downarrow}{d\sigma_\uparrow + d\sigma_\downarrow},$$

where $P_{\rm b}$ is the beam polarization value. Thus, the asymmetry is positive when particles tend to fly to the left when the beam polarization is directed upward.

The data used for this analysis were stored during the FNAL accelerator run in 1990 and contained about $6.6 \cdot 10^6$ events for $p_\uparrow p$ and $3.3 \cdot 10^6$ events for $\bar{p}_\uparrow p$ collisions written on data summary tapes.

The detector configuration is shown in Fig. 1. The Fermilab polarized beam facility is described elsewhere [5]. The polarized protons were obtained from the decay of Λ hyperons, and the proton polarization was determined by a tagging system of the particle trajectory. A set of spin-rotation magnets, a so-called "Siberian snakes", was used to change the polarization direction from the transverse-horizontal to the vertical one. Then the beam interacted with the 100 cm-long liquid-hydrogen target. Photons were detected by the electromagnetic calorimeter EC. The detector was assembled of lead-glass counters in the array of 21 columns by 24 rows. The size of each counter was $38.1 \times 38.1 \times 450$ mm^3.

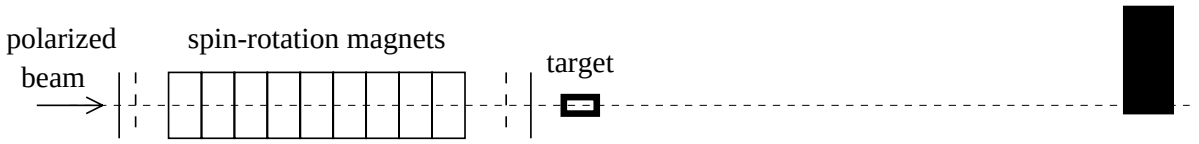

Fig. 1. The schematic layout of the E704 setup.

The energy resolution of the electromagnetic calorimeter (RMS) was $\Delta E/E = 0.01 \oplus 0.12/\sqrt{E\ [\mathrm{GeV}]}$. The detector was positioned at 10 m downstream from the target center and the beam axis came to the center of the middle counter of the first column. Such a configuration allowed one to accept the largest x_F range.

1. Algorithm of extracting η from data

All combinations of photon pairs plotted against the pair mass show a distinguished peak from the π^0-meson. But, due to the abundance of π^0's in each event in comparison with η's, the combinatorial background contaminates very much the peak in $\gamma\gamma$-spectrum at the η-meson mass, 547 MeV/c^2. The first step to have a clearer η-signal is to remove showers in the EC caused by hadrons which can be performed by the shower shape. Hadrons produce showers in a calorimeter with much larger fluctuations than photons do. As a criterium of a "good" electromagnetic shower a minimization of the parameter ρ, a type of χ^2, was used:

$$\rho = \frac{\left(\sum(E_{\mathrm{exp}} - E_0)\right)^2}{\sum E_{\mathrm{exp}}},$$

where the sum is given over all cells of the calorimeter, E_{exp} is a measured deposited energy in each lead-glass counter, and E_0 is the predicted deposited energy in each cell based on the average shower shape. Using the energy resolution of the calorimeter we can obtain the mean $\langle\rho\rangle = 0.014$ GeV for electromagnetic particles. We exclude all showers with $\rho > 0.05$ GeV from the data analysis as responses from hadrons. The rest of the showers are considered to be electromagnetic showers, or responses from photons.

To exclude the kinematical region with low asymmetry, we limit the transverse momentum of a shower pair by $0.7 < p_T < 2.0$ GeV/c. The mass-spectrum of the remaining shower pairs still has a large background under the η-peak. At the next step of the analysis, the photons originated from π^0-mesons are removed from further consideration. The π^0 candidates are chosen in the following way. For any photon pair the variable x_F is determined; for this x_F the minimum distance between photons from η-meson decay on the face of EC is determined as $\Delta_{\mathrm{min}} = 2z_{\mathrm{targ}}M_\eta/x_F p_{\mathrm{lab}}$, where z_{targ} is a distance between the target center and the detector and $M_\eta = 0.547$ GeV/c^2. All γ-pairs with the distance $\Delta < 0.6\Delta_{\mathrm{min}}$ are taken as π^0 candidates and omitted from further analysis. While no γ-pair from an η-meson has a distance on the EC face less than Δ, this algorithm of π^0 elimination rules out some number of η-mesons along with π^0's, because in the vicinity of γ from η a photon from π^0 can exist. Nevertheless, as it will be shown later, this method

does not change the measured asymmetry, and the combinations of the remained showers give a spectrum with a significantly improved peak at the η-meson mass. The unpolarized spectra of the two-photon masses in pp collisions at different x_F intervals are shown in Fig. 2; the specrta in $\bar{p}p$ collisions look analogously, but about 3 to 4 times lower.

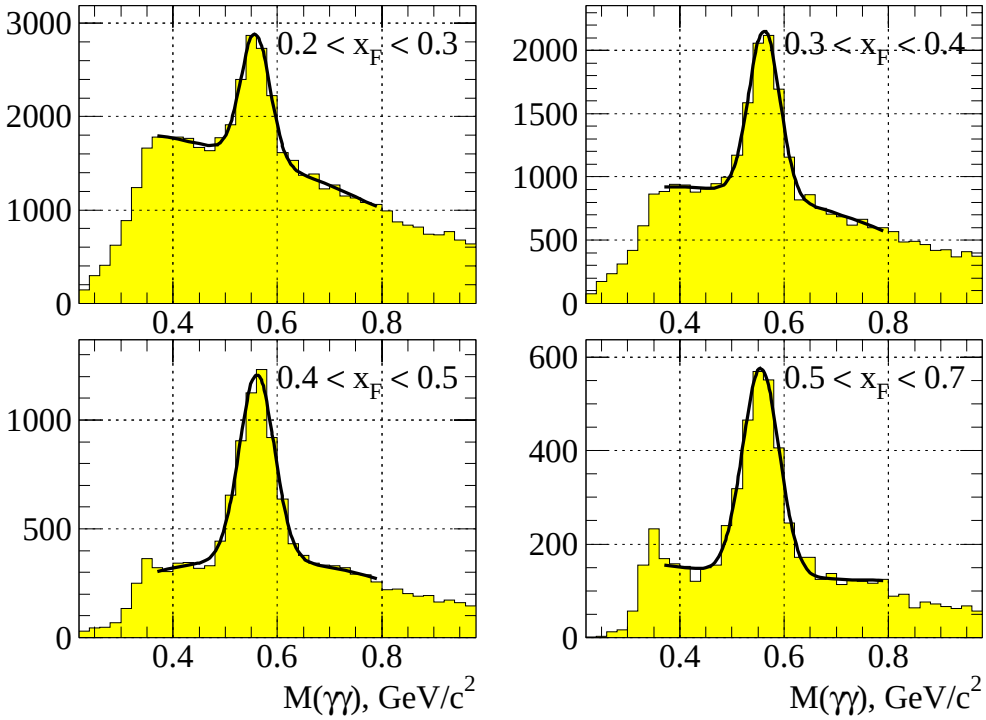

Fig. 2. The unpolarized two-photon spectra in $p_{\uparrow}p$ collisions after π^0 rejection at different x_F intervals and $0.7 < p_T < 2.0$ GeV/c.

2. Asymmetry in η-meson production.

To measure the spin asymmetry, two samples of events with opposite signs of the beam polarization $P = \pm(0.35 \text{ to } 0.65)$ with the average polarization $\langle P \rangle = \pm 0.46$ were taken. The distribution of the beam polarization is shown in Fig. 3, the dark area denotes the polarization used for the asymmetry measurement. The spin asymmetry was determined as a relative difference of cross-sections of these two samples. Simultaneously a check for systematic errors of the spin asymmetry was performed by determining the false asymmetry. The false asymmetry was determined with two other samples of events: having been integrated over the beam polarization $P = -0.35$ to $+0.35$ to obtain zero-polarization samples, events were split by the so-called "beam-spin-reversal-states", i. e. by two independent states of the spin-rotation magnets. Since these event samples are not correlated with the beam polarization, the false asymmetry should be zero in the absence of systematic errors.

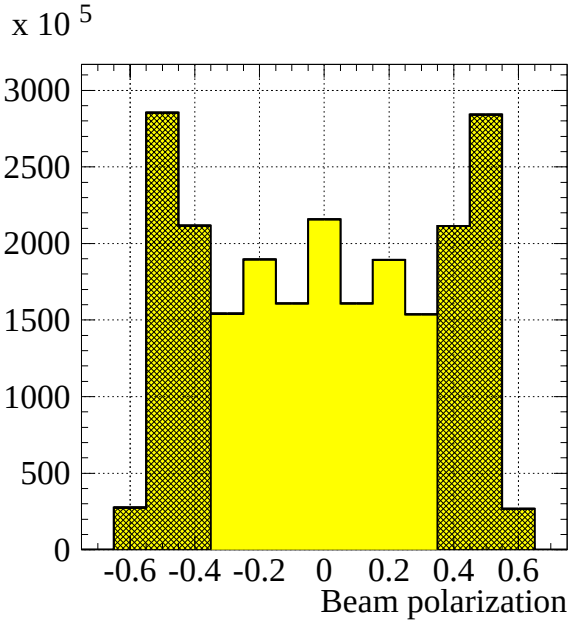

Fig. 3. Beam polarization distribution. The dark area shows the polarization used at the asymmetry measurement.

The cross section of photon-pair production with the invariant mass consistent with that of η-meson at fixed direction of the beam polarization is defined by the sum of the cross section of the η-meson itself and of the photon-pairs coming from the non-resonant background:

$$\sigma^{\pm}_{\gamma\gamma} = \sigma^0_\eta(1 \pm A_\eta) + \sigma^0_{\rm b}(1 \pm A_{\rm b}),$$

where σ^0_η and $\sigma^0_{\rm b}$ are unpolarized cross sections of η-meson and background, and A_η and $A_{\rm b}$ stand for their asymmetries. Hence, the asymmetry in η-meson production can be determined from the asymmetry $A_{\rm raw}$ of $\gamma\gamma$ pairs with masses including the η-peak in the mass spectra, the asymmetry $A_{\rm b}$, and the ratio B of unpolarized cross sections of the background two-photon pairs and the η-meson production ($B = \sigma^0_{\rm b}/\sigma^0_\eta$):

$$A_\eta = (1 + B)A_{\rm raw} - BA_{\rm b}.$$

Since the left-right asymmetry of particle production is proportional to the cosine of the azimuth angle ϕ, the data were split in 5 ϕ-bins, and the asymmetry parameter was defined as a proportionality coefficient between $\cos\phi$ and $A_N(\phi)$.

The asymmetry $A_{\rm raw}$ is measured directly from the two-photon mass spectra as the asymmetry in the $\gamma\gamma$-pair production with masses $480 < M_{\gamma\gamma} < 640$ MeV/c^2. The asymmetry $A_{\rm b}$ can be estimated by interpolating the asymmetries of nonresonant two-photon pairs around the η-meson mass into the mass region under the η-peak. The two first columns of the Table 1 and 2 show the true asymmetries in $p_\uparrow p$ and $\bar{p}_\uparrow p$ collisions of two-photon pairs with masses $480 < M_{\gamma\gamma} < 640$ MeV/c^2 ($A_{\rm raw}$) and two-photon pairs with masses around the η peak, $250 < M_{\gamma\gamma} < 420$ MeV/c^2 and $640 < M_{\gamma\gamma} < 900$ MeV/c^2 ($A_{\rm b}$) versus (x_F, p_T)-point.

The background ratio B is defined from the unpolarized mass spectra of two-photon combinations (Fig. 2). The spectra are fitted by the sum of the Gaussian distribution and the second-order polynomial

$$f(m) = A\exp\left(-\frac{(m-\bar{m})^2}{2\sigma^2}\right) + a_0 + a_1 m + a_2 m^2,$$

where the Gaussian describes $\gamma\gamma$-pairs from the η-meson and the polynomial describes nonresonant $\gamma\gamma$-pairs. The background B is the ratio of the two parts of the mass distribution integrated over the mass interval $480 < M_{\gamma\gamma} < 640$ MeV/c^2. The numerical

values of background ratios versus x_F for $p_\uparrow p$ and $\bar{p}_\uparrow p$ are represented in the third column of Tables 1 and 2.

Table 1. True asymmetries of $\gamma\gamma$-pairs $A_{\rm raw}$, $A_{\rm b}$, background ratio B, true and false asymmetries in η-meson production $A_\eta^{\rm true}$ and $A_\eta^{\rm false}$ versus (x_F, p_T) in $p_\uparrow p$ collisions.

x_F-range	$\langle x_F \rangle$	$\langle p_T \rangle$ GeV/c	$A_{\rm raw}$, %	$A_{\rm b}$, %	B	$A_\eta^{\rm true}$, %	$A_\eta^{\rm false}$, %
$0.2-0.3$	0.247	1.03	-1.4 ± 1.4	-0.7 ± 1.2	1.33 ± 0.09	-5 ± 8	0 ± 7
$0.3-0.4$	0.345	1.05	-0.5 ± 1.7	-2.8 ± 1.6	0.71 ± 0.07	2 ± 7	-1 ± 6
$0.4-0.5$	0.444	1.08	3.8 ± 2.2	-2.2 ± 2.4	0.40 ± 0.07	13 ± 7	-21 ± 6
$0.5-0.7$	0.562	1.09	8.0 ± 3.2	-4.9 ± 3.7	0.28 ± 0.08	25 ± 9	-12 ± 8

Table 2. True asymmetries of $\gamma\gamma$-pairs $A_{\rm raw}$, $A_{\rm b}$, background ratio B, true and false asymmetries in η-meson production $A_\eta^{\rm true}$ and $A_\eta^{\rm false}$ versus (x_F, p_T) in $\bar{p}_\uparrow p$ collisions.

x_F-range	$\langle x_F \rangle$	$\langle p_T \rangle$ GeV/c	$A_{\rm raw}$, %	$A_{\rm b}$, %	B	$A_\eta^{\rm true}$, %	$A_\eta^{\rm false}$, %
$0.3-0.4$	0.346	1.00	0.6 ± 2.5	-4.5 ± 2.2	0.71 ± 0.09	9 ± 10	5 ± 9
$0.4-0.5$	0.444	1.00	3.0 ± 3.6	-1.4 ± 3.8	0.54 ± 0.11	12 ± 13	-12 ± 11
$0.5-0.7$	0.560	1.03	-5.2 ± 5.9	6.3 ± 6.3	0.31 ± 0.15	-19 ± 17	24 ± 16

The defined values of the raw and background asymmetries and the background ratio now allow one to obtain the final result on the asymmetry in η-meson production. The true and false η-meson asymmetries $A_\eta^{\rm true}$ and $A_\eta^{\rm false}$ in terms of x_F are shown in Fig. 4 for $p_\uparrow p$ collisions and Fig. 5 for $\bar{p}_\uparrow p$ collisions; for convenience false asymmetries are shifted in x_F. The numerical values of $A_\eta^{\rm true}$ are given in the fourth column of Tables 1 and 2, those of $A_\eta^{\rm false}$ are shown in the last columns.

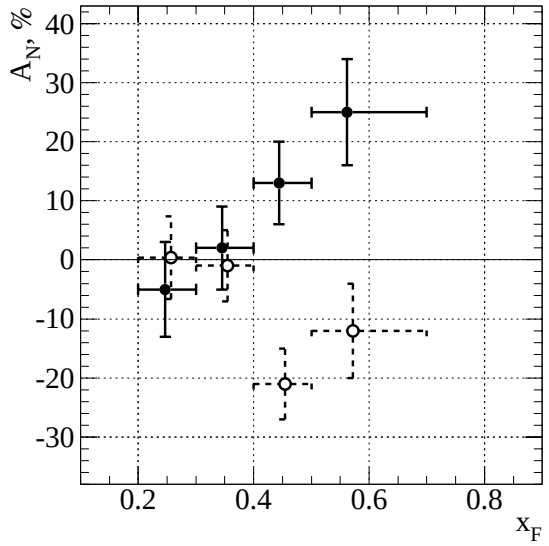

Fig. 4. True (solid lines) and false (dashed lines) asymmetries in η-meson production in $p_\uparrow p$ collisions versus x_F at $0.7 < p_T < 2.0$ GeV/c.

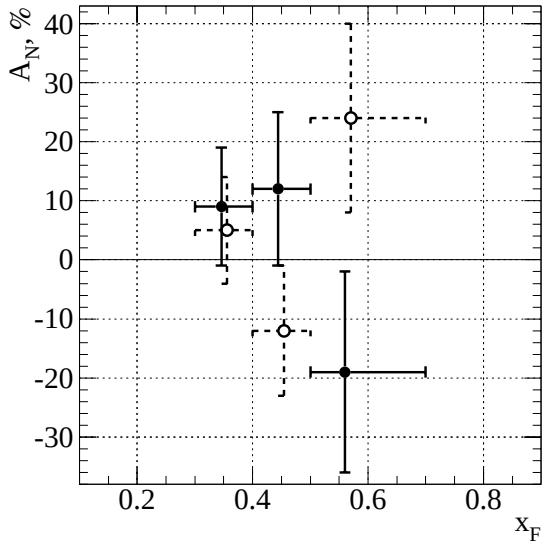

Fig. 5. True (solid lines) and false (dashed lines) asymmetries in η-meson production in $\bar{p}_\uparrow p$ collisions versus x_F at $0.7 < p_T < 2.0$ GeV/c.

To prove the validity of the algorithm chosen to extract η-meson spectra described in Section 1, we compare the result of these spectra and asymmetries before (set 1) and after (set 2) π^0 elimination. Tables 3 and 4 show the number of η-mesons N_η, background ratios B and asymmetry A_η of these two data sets in $p_\uparrow p$ and $\bar{p}_\uparrow p$ collisions. Here the number of η-mesons is found as an integral under the Gaussian peak of the unpolarized mass-spectra in Fig. 2. From this Table it follows that a significant number of η-mesons are lost after π^0-removal for $x_F < 0.5$ while the background is subtracted more by this algorithm. The asymmetry remains the same within the error bars.

Table 3. Number of η-mesons N_η, background ratio B and asymmetry A_η for data sets before (set 1) and after (set 2) π^0 elimination in $p_\uparrow p$ collisions.

x_F-range	N_η		B		A_η, %	
	set 1	set 2	set 1	set 2	set 1	set 2
$0.2-0.3$	$(25.6\pm0.9)\cdot10^3$	$(9.3\pm0.3)\cdot10^3$	3.68 ± 0.14	1.33 ± 0.09	-3 ± 6	-5 ± 8
$0.3-0.4$	$(18.6\pm0.7)\cdot10^3$	$(9.6\pm0.3)\cdot10^3$	1.97 ± 0.49	0.71 ± 0.07	-2 ± 6	2 ± 7
$0.4-0.5$	$(10.5\pm0.3)\cdot10^3$	$(7.0\pm0.2)\cdot10^3$	0.90 ± 0.07	0.40 ± 0.07	12 ± 6	13 ± 7
$0.5-0.7$	$(4.9\pm0.2)\cdot10^3$	$(3.9\pm0.1)\cdot10^3$	0.41 ± 0.08	0.28 ± 0.08	17 ± 8	25 ± 9

Table 4. Number of η-mesons N_η, background ratio B and asymmetry A_η for data sets before (set 1) and after (set 2) π^0 elimination in $\bar{p}_\uparrow p$ collisions.

x_F-range	N_η		B		A_η, %	
	set 1	set 2	set 1	set 2	set 1	set 2
$0.3-0.4$	$(7.5\pm0.3)\cdot10^3$	$(4.6\pm0.2)\cdot10^3$	1.80 ± 0.12	0.71 ± 0.09	5 ± 9	9 ± 10
$0.4-0.5$	$(3.3\pm0.2)\cdot10^3$	$(2.5\pm0.1)\cdot10^3$	1.06 ± 0.13	0.54 ± 0.11	14 ± 12	12 ± 13
$0.5-0.7$	$(1.5\pm0.1)\cdot10^3$	$(1.2\pm0.1)\cdot10^3$	0.47 ± 0.16	0.31 ± 0.15	-12 ± 16	-19 ± 17

Really, the method of the asymmetry measurement discussed above is irrelevant to the background level because the raw η-meson asymmetry is corrected by the background asymmetry. Both algorithms give almost equal results with equal errors. The comparison of the asymmetries of the two data sets indicates the stability of the asymmetry against the method of analysis. An alternative method of the asymmetry calculation based on the direct measurement of the η-meson cross section by fitting the polarized two-photon mass spectra results in the same values of the asymmetry but with higher errors, because the fit of poor-statistics mass spectra with an unknown form of the background has much higher errors than the statistical ones.

3. Discussion

The asymmetries in η-meson production have been measured. The asymmetry in η-meson production in $p_\uparrow p$ interactions shows the tendency to be positive and growing in the range $0.3 < x_F < 0.7$ and $0.7 < p_T < 2.0$ GeV/c. The averaged asymmetry over the region $0.4 < x_F < 0.7$, where the asymmetry deviates from zero-value by more than one

standard error, is $A_N = 17 \pm 5\%$. This result is proved by the consistency of the false asymmetry with zero.

The asymmetry in $\bar{p}_\uparrow p$ interactions does not permit to make a strict conclusion about its behaviour because of poor statistics. The average asymmetry over the region $0.4 < x_F < 0.7$, $0.7 < p_T < 2.0$ GeV/c is $A_N = 2 \pm 10\%$.

The systematic error of the asymmetry is significantly reduced due to the frequent change of the beam polarization. The main source of the systematic error is an uncertainty in the polarization measurement which results in the relative error of the asymmetry $\delta A_N / A_N = 0.12$. Another systematic error arises from the background ratio B determination. This error is smaller and it adds not more than 2% to the absolute error of the asymmetry.

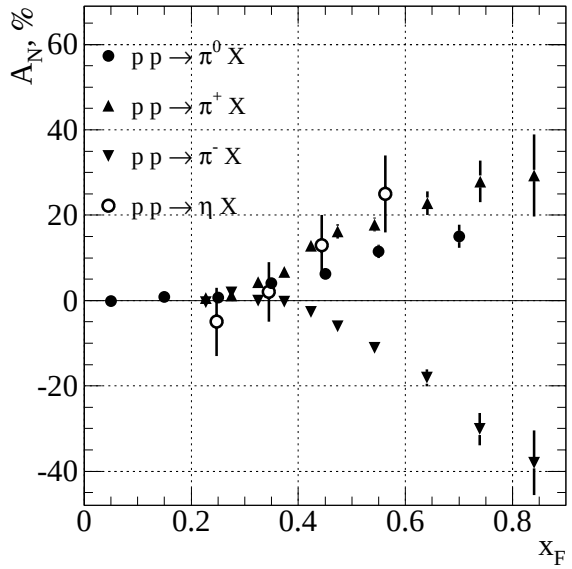

Fig. 6. The comparison plot of single spin asymmetries in the polarized proton beam fragmentation region.

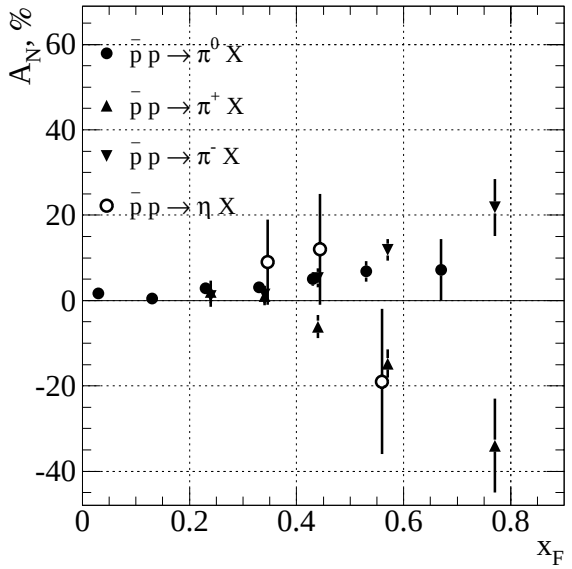

Fig. 7. The comparison plot of single spin asymmetries in the polarized antiproton beam fragmentation region.

As was mentioned earlier, the experiment E704 had measured single spin asymmetries in π-meson and Λ-hyperon production in the same kinematical region. Figs. 6 and 7 show the comparison plots of measured spin asymmetries in π^0, $\pi^\pm$ and η production in the fragmentation region of the polarized proton and antiproton beams. The asymmetries in π-meson production are much more statistically reliable. Nevertheless, one can say that the asymmetry of η-meson qualitatively behaves like that of π^0 and π^+ in $p_\uparrow p$-collisions. All the asymmetries are consistent with zero at small x_F, become non-zero at moderate x_F and grow towards the fragmentation region.

A successful description of the previous data on single spin asymmetries for pions and Λ-hyperons is given by the Berliner relativistic quark model [6]. The model is based on assumptions that most particles in the fragmentation region are formed by the valence quarks of the projectile; that the valence quarks are polarized in a polarized hadron;

and that the surface effect plays an important role in inclusive production processes. This model predicts also that the sign of the single spin asymmetry in inclusive η-meson production in the fragmentation region of the polarized projectile proton should be the same as that for π^0 and π^+, i. e. positive. This prediction is confirmed by the experimental measurement presented in the current publication.

Conclusion

We have presented the new result on the transverse single spin asymmetry measurement in η-meson production in $p_\uparrow p$ and $\bar{p}_\uparrow p$ interactions at $p_{\rm lab} = 200$ GeV/c at $0.2 < x_F < 0.7$ and $0.3 < x_F < 0.7$ respectively and p_T near 1 GeV/c. The result indicates that the asymmetry in $p_\uparrow p$-collisions is positive. The average value of the asymmetry over the x_F-region $0.4 < x_F < 0.7$ is $A_N = 17 \pm 5\%$. The asymmetry in $\bar{p}_\uparrow p$-interactions is consistent with zero. Within the error bars, the experimental result is consistent with the prediction of the Berliner model.

References

[1] D. L. Adams et al. Zeit. Phys. C56 (1992) 181.

[2] D. L. Adams et al. Phys. Lett. B264 (1991) 462;
A. Bravar et al. Phys. Rev. Lett. 77 (1996) 2626.

[3] A. Bravar et al. Phys. Rev. Lett. 75 (1995) 3073.

[4] J. Ashkin et al. Proc. of the Ann Arbor Workshop on Higher energy polarized proton beams. AIP Conference Proc. No.42. p. 142 (Ann Arbor) 1978.

[5] D. P. Grosnick et al. Nucl. Instr. Meth. A290 (1990) 269.

[6] Liang Zuo-tang and Meng Ta-chung, Z. Phys. A344, (1992) 171.
C. Boros, Liang Zuo-tang, Meng Ta-chung. Phys. Rev. Lett. 70 (1993) 1751.
C. Boros, Liang Zuo-tang, Meng Ta-chung. Phys. Rev. D51 (1995) 4698.
C. Boros, Liang Zuo-tang, Meng Ta-chung. Phys. Rev. D53 (1996) 2279 R.
C. Boros, Liang Zuo-tang, Meng Ta-chung. Phys. Rev. D54 (1996) 4680.

Received August 21, 1997

FNAL E704 Collaboration

D. L. Adams, B. E. Bonner, M. D. Corcoran, J. Cranshaw, M. Nessi[a], F. Nessi-Tedaldi[b], C. Nguyen[c], J. B. Roberts, J. Skeens, J. L. White[d]
T.W.Bonner Nuclear Laboratory, Rice University, Houston, TX 77251, USA

N. Akchurin, Y. Onel
Department of Physics, University of Iowa, Iowa City, IA 52242, USA

L. V. Alexeeva, N. I. Belikov, A. A. Derevschikov, O. A. Grachov, Yu. V. Kharlov, Yu. A. Matulenko, A. P. Meschanin, L. V. Nogach, S. B. Nurushev, D. I. Patalakha, V. L. Rykov[e], V. L. Solovyanov, A. N. Vasiliev
Institute for High Energy Physics, Protvino, 142284, Russia

J. Bystricky, F. Lehar, A. de Lesquen
CEN-Saclay, F-91191 Gif-sur-Yvette, France

J. D. Cossairt, A. L. Read, L. van Rossum
Fermi National Accelerator Laboratory, Batavia, IL 60510, USA

H. En'yo, H. Funahashi, Y. Goto[f], T. Iijima[g], K. Imai, Y. Itow[h], S. Makino[i], A. Masaike, K. Miyake, T. Nagamine[j], N. Saito[f], S. Yamashita[k]
Department of Physics, Kyoto University, Kyoto 606, Japan

D. P. Grosnick, D. A. Hill, K. W. Krueger, M. Laghai, D. Lopiano, Y. Ohashi[l], T. Shima, H. Spinka, R. W. Stanek, D. G. Underwood, A. Yokosawa
Argonne National Laboratory, Argonne, IL 60439, USA

K. Iwatani
Hiroshima University, Higashi-Hiroshima 724, Japan

K. Kuroda, A. Michalowicz
Laboratoire de Physique des Particules, B.P.909, F-74017 Annecy-le-Vieux, France

F. C. Luehring[a], D. H. Miller
Physics Department, Northwestern University, Evanston, IL 60201, USA

T. Maki
University of Occupational and Environmental Health, Kita-Kyushu 807, Japan

G. Pauletta
University of Udine, I-33100 Udine, Italy

A. Bravar[m], A. Penzo, P. Schiavon, A. Zanetti
Dipartimento di Fisica, Universita di Trieste, I-34100 Trieste, Italy

G. F. Rappazzo, G. Salvato
Dipartimento di Fisica, Universita di Messina, I-98100 Messina, Italy

R. Takashima
Kyoto University of Education, Kyoto 612, Japan

F. Takeutchi
Kyoto-Sangyo University, Kyoto 612, Japan

N. Tamura[n]
Okayama University, Okayama 700,Japan

N. Tanaka[o]
Los Alamos National Laboratory, Los Alamos, NM 87545, USA

T. Yoshida
Osaka City University, Osaka 558, Japan

[a]Present address: Indiana University, Bloomington, IN 47405, USA.
[b]Present address: CERN, CH-1211 Geneva 23, Switzerland.
[c]Present address: University of Texas, Austin, TX 78712, USA.
[d]Present address: American University, Washington, D.C. 20016, USA.
[e]Present address: Wayne State University, Detroit, MI 48201, USA.
[f]Present address: Radiation Laboratory, Riken, Saitama 351-01, Japan.
[g]Present address: National Laboratory for High Energy Physics (KEK), Japan.
[h]Present address: Institute for Cosmic Ray Research, University of Tokyo, Gifu 506-12, Japan.
[i]Present address: Wakayama Medical College, Wakayama 649-63, Japan.
[j]Present address: Bubble Chamber Physics Laboratory, Tohoku University, Sendai 980, Japan.
[k]Present address: International Center for Elementary Particle Physics (ICEPP), University of Tokyo, Tokyo 113, Japan.
[l]Present address: Japan Synchrotron Radiation Research Institute, Hyogo, 678-12, Japan.
[m]Present address: Universität Mainz, D-55099, Germany.
[n]Present address: Graduate School of Science and Technology, Niigata University, Niigata 950-21, Japan.
[o]Deceased.

Коллаборация E704, ФНАЛ
Измерение односпиновой симметрии в образовании η-мезона в $p_\uparrow p$- и $\bar{p}_\uparrow p$-взаимодействиях в области фрагментации пучка при 200 ГэВ/с.

Оригинал-макет подготовлен с помощью системы LaTeX.
Редактор Е.Н.Горина. Технический редактор Н.В.Орлова.

Подписано к печати 22.08.97. Формат 60 × 84/8. Офсетная печать.
Печ.л. 1.25. Уч.-изд.л. 1.05. Тираж 240. Заказ 1083. Индекс 3649.
ЛР №020498 17.04.97.

ГНЦ РФ Институт физики высоких энергий
142284, Протвино Московской обл.

Индекс 3649

П Р Е П Р И Н Т 97–56, И Ф В Э, 1997